Water Practice & Technology

IWA PUBLISHING

Water Practice & Technology Vol 19 No 9, 3439 doi: 10.2166/wpt.2024.232

Response of remote sensing-based climatic indicators to drought conditions during El Niño events and implications for water–food–energy nexus

Kawawa Banda[a,*], Micheal Katongo Phiri[a,b] and Imasiku Nyambe[a]

[a] Integrated Water Resources Management Centre, Department of Geology, School of Mines, University of Zambia, Great East Road Campus, P.O. Box 32379, Lusaka 10101, Zambia
[b] National Remote Sensing Centre, Airport Road, Chelstone, P.O. Box 31030, Lusaka 10101, Zambia
*Corresponding author. E-mail: kawawa.banda@unza.zm

KB, 0000-0001-7083-3014

ABSTRACT

Hydrometeorological extremes, such as droughts, are a major threat to society and can have extensive damaging effects. In this study, daily rainfall estimates from the Climate Hazards Group InfraRed Precipitation with Stations (CHIRPS) quasi-global rainfall dataset were used to calculate the Standardised Precipitation Index (SPI) for the assessment of meteorological drought in Southern Province, Zambia. Normalised Difference Vegetation Index (NDVI) imagery (250 m resolution) from MODIS-Terra, for the period 2000–2021, were used to derive the Standardised Vegetation Index (SVI) in order to assess agricultural drought. The Mann–Kendall trend test and Sen's slope were used to determine the spatial-temporal trends and their magnitudes. This study demonstrated that the droughts of the Southern Province of Zambia can be classified into two categories: regressive and aggressive droughts. Regressive droughts are associated with moderate to strong El Niño events. Although El Niño events undermine water security, regressive droughts tend to result in resilient vegetation owing to residue soil moisture. In contrast, aggressive droughts are characterised by an increase in drought intensity as the season progresses. Water security prospects in the region should focus on climate-smart approaches, such as managed aquifer recharge, to ensure water availability even under extreme drought conditions.

Key words: drought, NDVI, Southern Province, SPI, SVI, Zambia

HIGHLIGHTS

- SPI, NDVI, and SVI can track El Niño events.
- SVI tends to be resilient owing to the soil moisture conditions during El Niño events.
- El Niño events can be classified as aggressive or recessive depending on the strength.
- Strong El Niño events tend to recede by February compared with weak moderate ones.
- Extreme drought events require appropriate water–food nexus actions which can be informed by the remote sensing indices.

GRAPHICAL ABSTRACT

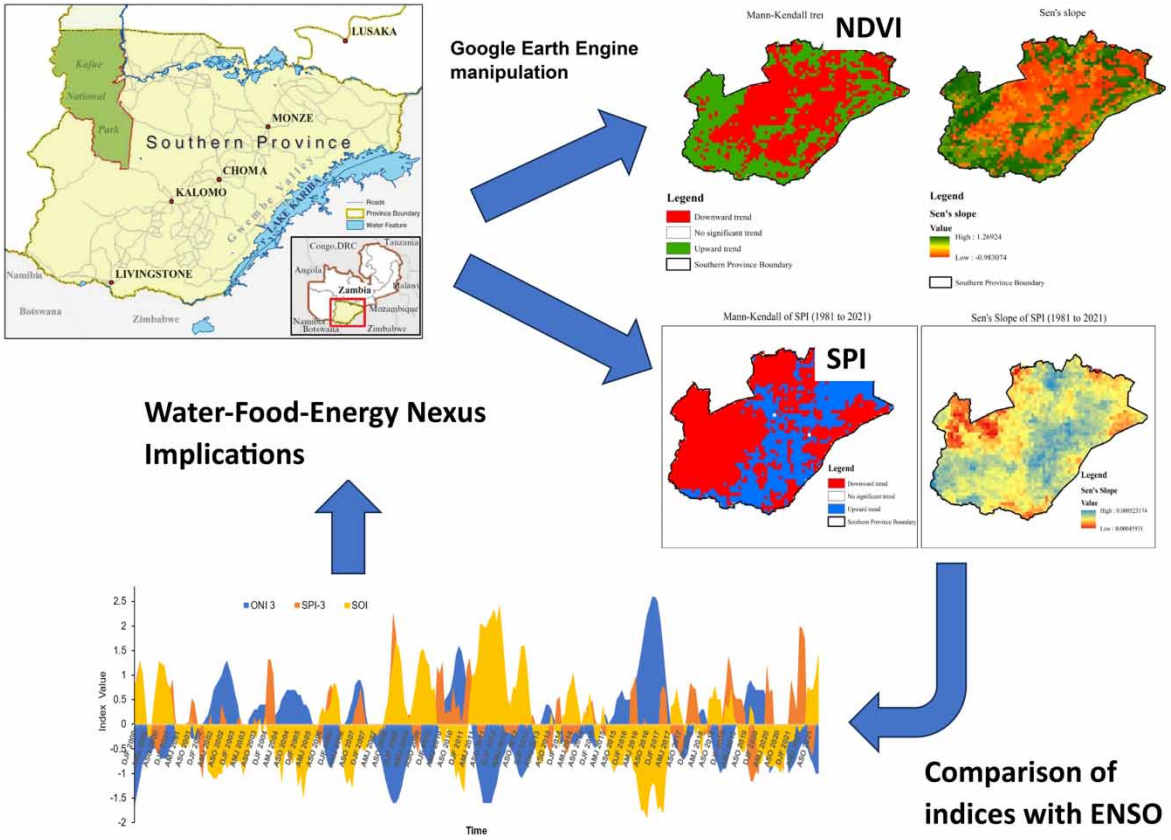

ABBREVIATIONS

ENSO	El Niño Southern Oscillation
NDVI	Normalised Difference Vegetation Index
ONI	Oceanic Niño Index
SPI	Standardised Precipitation Index
SVI	Standardised Vegetation Index
VCI	Vegetation Condition Index
WEF	Water–energy–food nexus

1. INTRODUCTION

Droughts are a recurring, complex, creeping hydrometeorological phenomenon, which unpredictably occurs as a result of water availability deficiency from rainfall amounts below the usual average (Dai 2011; Van Loon *et al.* 2016; Mikaili & Rahimzadegan 2022). During droughts, the manner in which dry conditions propagate deficits in soil moisture, runoff, and recharge is complex and heterogeneous across geographical domains (Raposo *et al.* 2023). Future climate change predictions suggest that many areas will start to experience more frequent and intense dry conditions with irreversible impacts for people and ecosystems (IPCC 2014). Many countries, particularly those whose economies rely significantly on rain-fed agriculture, are vulnerable to the effects of climate variability and change. This is the situation in most African countries (Niang *et al.* 2014). Unfortunately, the majority of these countries are extremely vulnerable to climate change and have limited adaptive capacity to cope with the impacts of climate change (Dibi-Anoh *et al.* 2023; Taye & Dyer 2024).

Droughts are broadly categorised into four groups: meteorological, agricultural, and hydrological. Meteorological droughts are quite common, and they are primarily classified by the extent of dryness in a given location and the length of the dry period. Although agricultural droughts are linked to a lack of water needed to support crops, the drought does not always coincide with meteorological drought. On the other hand, hydrological drought is

limited to the level of streamflow that can meet the demand. A study by Wilhite & Glantz (1985) gives a detailed description of this specific drought phenomenon. Although droughts can end by sudden extreme precipitation, the precise termination point is contested, making the phenomenon difficult to quantify and analyse (such as West *et al.* 2019; Ayugi *et al.* 2022).

For detection and determination of drought, different methods are proposed, of which some methods are based on using information of meteorological stations. Based on this information, some meteorological drought indices are calculated such as Palmer Drought Severity Index (PDSI), Surface Water Supply Index (SWSI), Percent of Normal (PN) Index, and Standardised Precipitation Index (SPI). The last one is used more frequently (Bonaccorso *et al.* 2003; Zhang *et al.* 2012; Bhunia *et al.* 2020). The SPI (McKee *et al.* 1993) was developed for the purpose of assigning a single value to precipitation that can be compared across regions with different climates. The limited number of hydrometeorological stations in developing countries leads to data gaps restricting usage of ground-based data in drought risk decision support in developing countries. Another category of drought monitoring methods are those based on the calculation of vegetation indices by satellite imagery (Heim 2002; Bhuiyan *et al.* 2006; Ezzine *et al.* 2014; West *et al.* 2019; Fatras *et al.* 2021; Juntakut *et al.* 2021; Mikaili & Rahimzadegan 2022). Some other remote sensing drought assessment methods used soil moisture data (Souza *et al.* 2018; Fatras *et al.* 2021; Souza *et al.* 2021). Furthermore, using remote sensing datasets, evapotranspiration models or water balance models (Khalili *et al.* 2011; Zhang *et al.* 2019; Tam *et al.* 2023) have been used to assess droughts.

Numerous studies have been conducted on droughts using satellite-derived indices under various climatic and environmental conditions. Ji & Peters (2003) derived a Normalised Difference Vegetation Index (NDVI) from the Advanced Very High Resolution Radiometer (AVHRR) and SPI to monitor moisture-related vegetation conditions. They found that the 3-month SPI had the best correlation with the NDVI, indicating the effects of lag time and cumulative precipitation on vegetation. The lag time was likely due to variations in the vegetation type and soil properties. These findings corroborate those of Wilhite *et al.* (2000) and Morid *et al.* (2006), who showed that the SPI is more reliable at detecting emerging droughts than other meteorological indices, and is thus a useful tool for initiating mitigation and response actions. Ji & Peters (2005) investigated the relationship between NDVI and precipitation to evaluate the vegetation-climate interactions on a large scale. They found that the time lag was shorter in the early growing season but longer in the mid- to late-growing season. Jain *et al.* (2010) used the SPI, NDVI, Water Supply Vegetation Index (WSVI), and Vegetation Condition Index (VCI) for drought monitoring in the three districts of Bhilwara, Kota, and Udaipur in India using AVHRR satellite data. They showed that NDVI and WSVI were highly correlated with SPI at different timescales (1–9 months) across districts. Gebrehiwot *et al.* (2011) used SPI and VCI for the spatial and temporal assessment of meteorological and agricultural drought indices. The results of the analysis revealed the occurrence of drought in southern and eastern Ethiopia. Furthermore, a lag time was observed between the VCI peak and rain gauge stations; the monthly VCI and precipitation data 2 months later had a good correlation.

Thavorntam *et al.* (2015) used the SPI and VCI to assess and evaluate drought indices in vegetated areas. They used precipitation data from 1980 to 2009 and MODIS-Terra vegetation (MOD13Q1) datasets from 2001 to 2009. SPI analysis revealed drought events at 3 and 6 months in the central and northeastern parts of Thailand. They showed that the relationship between the VCI and SPI can be used to forecast drought in the subsequent few months. Ghazaryan *et al.* (2020) evaluated the effects of drought on remotely sensed parameters at various stages of crop growth. They calculated several indices, including the NDVI, Normalised Difference Moisture Index (NDMI), Land Surface Temperature (LST), and Tasseled Cap, using Sentinel-1-based backscattering intensity. They revealed that all the remotely sensed variables respond differently to drought conditions. Recently, Mikaili & Rahimzadegan (2022) used satellite vegetation indices, including the Modified Perpendicular Drought Index (MPDI), VCI, Normalised Difference Vegetation Index Anomalies (NDVIA), and Standardized Vegetation Index (SVI), to monitor agricultural drought at a local scale in semi-arid Iran. The VCI exhibited the highest capability for investigating agricultural droughts in different climatic regions. Furthermore, the vegetation indices had the highest correlation with 3-month lag time on the SPI timescale. Arab & Ahamed (2023) demonstrated the use of the SVI and SPI for near real-time drought monitoring and assessment.

Previous studies have shown that although numerous satellite indices have been introduced to assess drought parameters, SPI- and NDVI-related indices are predominantly used. Further, the performance of different satellite indices and the lag time between meteorological drought as well as its effect on vegetation cover (agricultural

drought) varies across different climatic and environmental conditions. Although the connection between droughts and climate variability and change has been examined in previous studies (e.g. Zhai *et al.* 2010; Zhang *et al.* 2012; Asadi-Zarch *et al.* 2015), the spatial-temporal and areal extent characteristics of rainfall anomalies during periods categorised as drier than normal (induced by the El Niño Southern Oscillation (ENSO) Phenomena) have not been thoroughly analysed (Hernández & Heslar 2019; Bhunia *et al.* 2020; Nikraftar *et al.* 2021; Dibi-Anoh *et al.* 2023).

The main contribution of this study was the use of common satellite indices (SPI and NDVI-based SVI) to evaluate the effects of El Niño on drought (onset, development, and termination) at a local scale. This assessment was conducted in Southern Province, Zambia, a semi-arid region which is highly vulnerable to drought. Adaptive actions under droughts are also proposed. The main objective of the study was therefore to investigate the response of remote sensing-based climatic indicators towards extreme drought conditions driven by El Niño. Specifically, it investigates (i) the trends of precipitation and vegetation using the satellite indices, (ii) evaluates how satellite indices respond spatio-temporally during extreme conditions, and (iii) explores actions to ensure water and food security during droughts.

2. MATERIALS AND METHODS

2.1. Study area

Southern Province, Zambia was selected as the study area (Figure 1). Southern Province is covered by two of Zambia's four agroecological zones: Region I and Region II. Agroecological Region I stretches laterally to the western and southern parts of the province, along the Zambezi and the Luangwa escarpments. The region consists of valleys and plains that are less than 1,000 m above sea level and it has limited production potential owing to poor sandy soils. The average annual rainfall is less than 800 mm, and the growing season lasts only 90–120 days (Waldman *et al.* 2019). Furthermore, the temperatures are relatively higher than those in other parts of the country. The region is most suitable for the small-scale farming of drought-resistant crops, such as millet, sorghum, sesame, and cotton (Waldman *et al.* 2019). Agroecological Region II consists of the central plateau area of the province, with elevations varying from 1,000 to 1,400 m. Annual rainfall is between 800 and 1,000 mm, and the growing season ranges from 120 to 160 days, which supports the growth of medium- to long-term crop varieties. Along with the central and eastern plateaus, the southern plateaus are considered to have the best agricultural potential in Zambia because they are suitable for the growth diverse base of primarily rain-fed crops and livestock production. The land is covered with fertile soils that support maize, wheat, soybeans, and tobacco.

Figure 1 | Location of Southern Province, Zambia (Map adapted from Cliggett *et al.* (2007)).

2.2. Data types and sources

The primary data source was the MOD13Q1.006 Terra Vegetation Indices 16-Day Global 250 m product from the Moderate-Resolution Imaging Spectroradiometer (MODIS). The data were based on NDVI and ranged from the 18th of February 2000 to the 23rd of April 2021. We utilised the NDVI data for trend analysis and to determine the SVI. The data were accessed using the Google Earth Engine (GEE) Platform. Climate Hazards Group InfraRed Precipitation with Stations (CHIRPS) data (1 January 1981 to 31 March 2021) were accessed from GEE. The data had a daily temporal resolution and a 0.05° spatial resolution. The CHIRPS data incorporate *in-situ* meteorological station data and satellite imagery. The data were used to calculate the SPI and for trend analysis.

2.3. Data processing and analysis

All the data processing and analyses were performed using the GEE Platform. The SPI and SVI were calculated using MOD13Q1.006 (NDVI) and CHIRPS, respectively, using the UN-SPIDER recommended GEE practices for SVI and SPI, following the recommended GEE practices of the United Nations Platform for Space-based Information for Disaster Management and Emergency Response. Trend analysis was performed for NDVI, precipitation, SPI, and SVI. Furthermore, statistical analysis was conducted using Minitab Version 18 software. All datasets used are available via the Earth Engine Data Catalogue (https://developers.google.com/earth-engine/datasets/catalog: Accessed 8th August 2022).

2.3.1. Calculation of SPI

The SPI for each daily CHIRPS pixel covering the Southern Province was calculated using GEE. The SPI is a meteorological drought index that was developed by McKee *et al.* (1993) for the purpose of assigning a single value to precipitation, enabling comparisons among regions with different climates. It is defined as the difference in precipitation from the mean for a defined time period divided by the standard deviation, where the mean and standard deviation are determined from past records (McKee *et al.* 1993). Therefore, SPI was derived using the following equation (McKee *et al.* 1993):

$$\mathrm{SPI} = (P_i - P_m)/\sigma \tag{1}$$

where P_i is the monthly precipitation, P_m is the long-term mean precipitation, and σ is the standard deviation of the long-term record.

In this study, the predefined time steps chosen were the SPI at 1 month and a 16-day SPI to match the MODIS vegetation index temporal resolution. However, because a lag exists between rainfall conditions and vegetation response (Thenkabail *et al.* 2004), the 16-day moving window was set to begin 7 days before the vegetation index collection dates. Therefore, the SPI began calculating 7 days before the MODIS start dates and ended 7 days earlier than the MODIS end dates. As cumulative rainfall for a period of less than 1 year tends to not be normally distributed, the rainfall data were normalised using the gamma probability density function. A fitted function was used to calculate the cumulative distribution of the data points. Finally, the data points were transformed into standardised normal variates using Equation (1). The SPI was classified into different drought categories of drought (Table 1) as prescribed by Stricevic *et al.* (2011).

Table 1 | SPI values and classification

SPI value	Interpretation
2.0 +	Extremely wet
1.5 to 1.99	Very wet
1.0 to 1.49	Moderately wet
−0.99 to 0.99	Near normal
−1.49 to −1.0	Moderately dry
−1.99 to −1.5	Severely dry
−2 and less	Extremely dry

According to previous studies (Wu *et al.* 2007; Mishra & Nagarajan 2011), the first limitation of the SPI is the length of the precipitation record, which has a significant impact on the SPI values. Therefore, the SPI can produce different results with different lengths of precipitation records. The second limitation is the probability distribution. Different probability distributions have been used in SPI calculations, namely gamma and Pearson Type III distribution, lognormal, extreme value, and exponential distributions, and have been widely applied to simulations of precipitation distributions (Wu *et al.* 2007). Another disadvantage is that when applying SPI at short timescales (1, 2, or 3 months) to regions with low seasonal precipitation, misleadingly large positive or negative SPI values may result.

2.3.2. Calculation of SVI

SVI was developed by Peters *et al.* (2002). It is an NDVI-based index used to assess relative vegetation conditions as it describes the probability of variation from normal NDVI over a number of years at a weekly time step. Therefore, the SVI is the z-score deviation from the mean (in standard deviation units) calculated for each pixel over a given study period (Peters *et al.* 2002), and this z-score is given by the following equation:

$$z_{ijk} = \frac{\mathrm{NDVI}_{ijk} - \overline{\mathrm{NDVI}_{ij}}}{\sigma_{ij}} \tag{2}$$

where z_{ijk} is the z-value of pixel i during week j for year k, NDVI_{ijk} is the weekly NDVI value of pixel i during week j for year k, $\overline{\mathrm{NDVI}_{ij}}$ is the average NDVI value of pixel i during week j over n years, and σ_{ij} is the standard deviation of pixel i during week j over n years.

The z-value was assumed to fit a standard normal distribution that has a mean of zero and a standard deviation of 1. To test this assumption, Peters *et al.* (2002) randomly selected from the 1989 to the 2000 growing season, and using the Shapiro–Wilk W-test, found that 80.3% of the pixels were normally distributed. Hence, Peters *et al.* (2002) formulated the following density probability function for z_{ijk} that gives the SVI:

$$\mathrm{SVI} = P(Z < z_{ijk}) \tag{3}$$

The SVI is calculated based on probability estimate to predict and visualise the relative vegetation greenness with reference to the greenness probability for each pixel, which infers a temporal comparison (Peters *et al.* 2002). As the index is NDVI-based, it is related to the red and near-infrared reflectance wavebands sensed and recorded by several Earth observation satellite platforms. Therefore, data to derive the SVI are readily available and can be accessed in near real time, making it suitable for monitoring temporal phenomena such as drought. As SVI is a temporal comparison of NDVI, a maximum-value composite approach based on time-series NDVI was used. Before calculating the SVI, data preparation and preprocessing were conducted, which involved the selection of a timeframe, cloud masking, resampling and rescaling of data, and clipping of the imagery to the boundaries of Southern Province. The z-values and SVI of each pixel were calculated using Equations (2) and (3), respectively.

2.4. Trend analysis

The Mann–Kendall trend test and Sen's slope method were used to perform the trend analysis. The Mann–Kendall trend test is used to determine whether a time-series dataset has a monotonic upward or downward trend. It is a nonparametric test; therefore, it does not require the data to be normally distributed or linear. Meanwhile, Sen's slope is a nonparametric test based on Kendall's rank correlation, tau. It is a point estimator for the median of a set of slopes $(Y_j - Y_i)/(t_j - t_i)$ joining pairs of points $t_j \neq t_i$ (Sen 1968). The Mann–Kendall trend test only provides an indication of an existing trend (upward or downward), whereas Sen's slope provides the magnitude.

Trends in rainfall, meteorological drought (SPI), and relative vegetation conditions were checked for each season. Despite conducting an analysis of the entire rainfall dataset (1981 to 2021), trend analysis was performed only from 2000 to 2021 to match with the timeframe of the MODIS-Terra vegetation indices. Furthermore, rainfall and SPI were aggregated into 16-day values (with start dates 7 days prior to accommodate the lag of the vegetation response) to match the NDVI and SVI dates. Trend analysis of rainfall was performed on a monthly basis; only the 16-day rainfall data of a particular month were considered in the trend analysis to compensate for

seasonality. Particular attention was paid to drought seasons with medium to strong El Niño patterns to check whether there were any differences between such droughts and those with an absent or weak El Niño pattern.

3. RESULTS AND DISCUSSION

3.1. Trends in precipitation and SPI during El Niño events

Analysis of the CHIRPS data for Southern Province revealed that the SPI was low in the rainy seasons of 2001/2002, 2002/2003, 2004/2005, 2013/2014, 2015/2016, and 2019/2020 (Figure 2). The 2001/2002 season had a severe drought, with an SPI value as low as −1.20 (moderately dry) and monthly rainfall values of 118, 155, 107, 64, and 37 mm in November 2001, December 2001, January 2002, February 2002, and March 2002, respectively. During 2001/2022, there were no prevailing El Niño conditions (Pomposi *et al.* 2018) and the rainfall trended downwards. In the present study, this type of drought was classified as aggressive. During the 2004/2005 season, weak El Niño conditions prevailed, and drought conditions worsened as the season progressed. Therefore, the drought during this season was also classified as aggressive. During the 2002/2003 season, moderate El Niño conditions prevailed (Waldman *et al.* 2019). In particular, the sea surface temperatures (SSTs) for the Niño 3.4 region were higher than normal (exceeding +0.4 °C for a period of 6 months or more). In this season, the SPI increased from −0.82 in November 2002 to −0.72 in December 2002. The SPI continued to rise as the season progressed and was −0.40 in February 2003 and 0.81 in March 2003. Similarly, rainfall increased from 47.52 mm in November 2002 to 111.03 mm in December 2002, 113.44 mm in January 2003, and 128.449 mm in February 2003 and dropped slightly to 122.28 mm in March 2003. According to the SPI, drought conditions improved as the 2002/2003 drought season progressed. In the present study, this type of drought was classified as regressive. The 2015/2016 drought season (classified as a strong El Niño event (Pomposi *et al.* 2018)) was similar to that of the 2002/2003 in that strong El Niño conditions were present and the drought conditions improved from severe to normal as the season progressed; therefore, the drought was also classified as regressive. In particular, in 2015, SSTs were higher than normal in the Niño 3.4 region, with the 3-month average of the Niño 3.4 index (referred to as the Oceanic Niño Index (ONI)) being as high as an average of 2.5 for October, November, and December (OND) (NOAA 2022). In this season (2015/2016), the SPI increased from −0.92 in November 2015 to 2.21 in March 2016 (Figure 2). In seasons where El Niño conditions prevailed, rainfall and SPI were low during November, December, and part of January, when El Niño signals tended to be the strongest, owing to a strong or moderate El Niño pattern. A correlation analysis of ONI and the Southern Oscillation Index (SOI) to the average 3-month SPI (SPI-3) showed a statistically significant correlation of −0.514 with ONI (Figure 3). The SOI, a sea surface pressure-dependent ENSO indicator, did not perform as well.

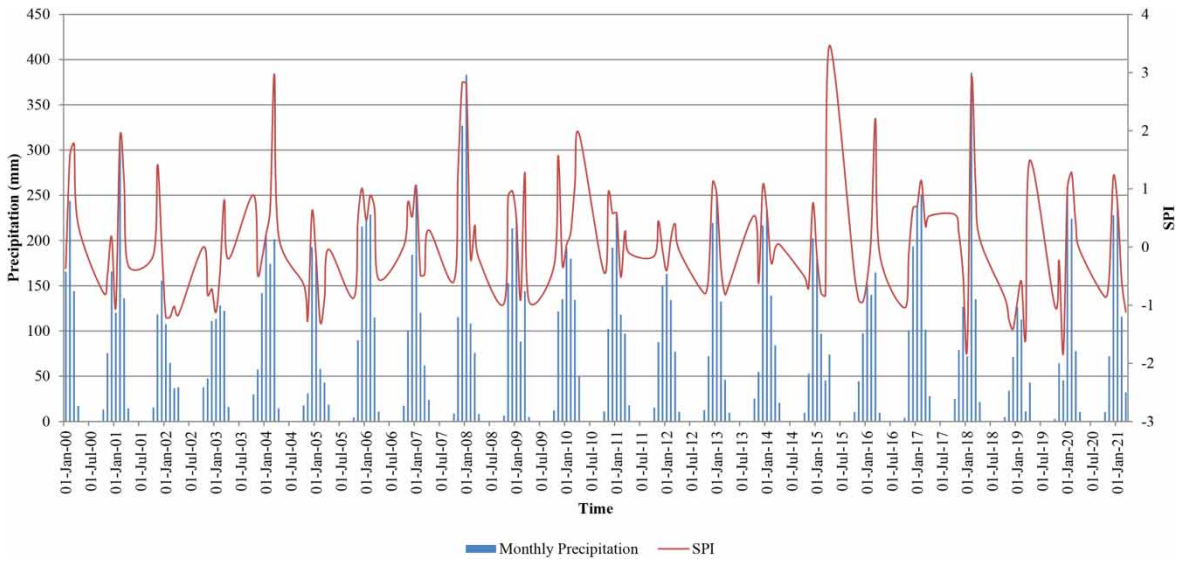

Figure 2 | Changes in monthly rainfall and SPI from January 2000 to March 2021 over the Southern Province of Zambia.

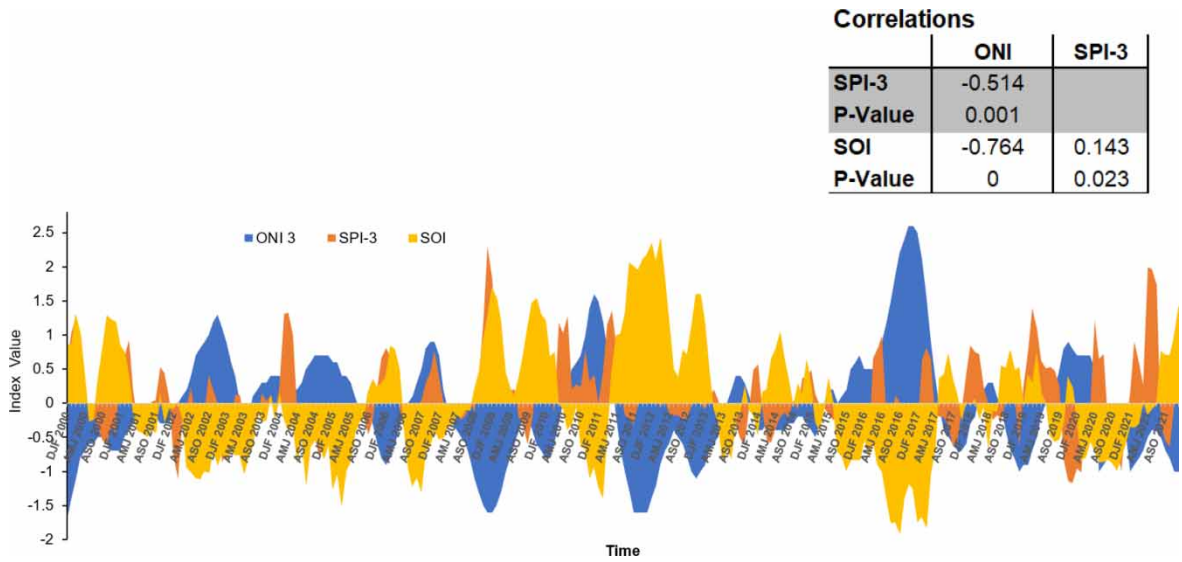

Figure 3 | Graph of ENSO indicators (ONI, SOI) with SPI-3 and Spearman correlation analysis.

In seasons where the El Niño conditions prevailed due to a strong or moderate El Niño signal, SPI was low in November, December, and part of January. Based on the Mann–Kendall trend test, the SPI of Southern Province displayed a downward trend during aggressive droughts and an upward trend during regressive droughts. Figure 4 shows the Mann–Kendall trend test results for the monthly SPI (with a 16-day moving window) during the 2001/2002 and 2015/2016 seasons. For the 2015/2016 rainfall season, approximately 98.96% of the province displayed an upward trend in the SPI, whereas only 0.48% displayed a downward trend. Approximately 0.56% of the province showed no distinct trend. This pattern is in line with the characteristics of regressive droughts, in which drought intensity decreases as the season progresses. Regarding the 2001/2002 rainfall season, 98.18% of the province showed a marked downward trend in the SPI as the season progressed. This was in line with the characteristics of aggressive droughts, in which the drought intensity increases as the season progresses.

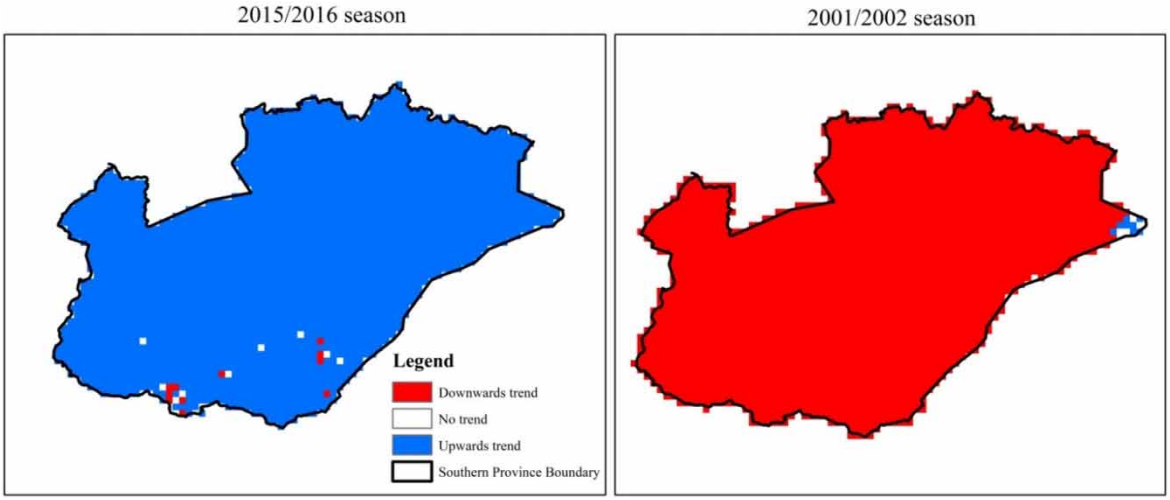

Figure 4 | Mann–Kendall trend tests for the 2001/2002 and 2015/2016 rainfall seasons.

Throughout the entire coverage of CHIRPS (1 January 1981 to 31 March 2021), the SPI showed an upward trend in the central regions of the province (mainly agroecological Region II) and a downward trend in the western regions (agroecological Region II) (Figure 5). Sen's slope revealed that the trends, both upward and downward, were very small. The largest upward trend had a median slope of 0.00052, whereas the lowest

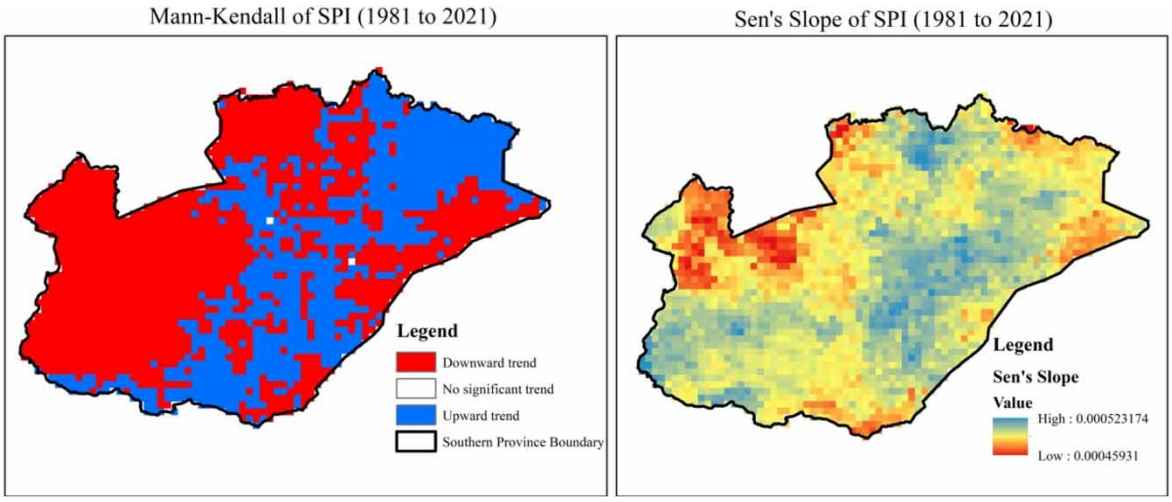

Figure 5 | Mann–Kendall trend test and Sen's slope of SPI for the Southern Province of Zambia between 1981 and 2021.

slope was 0.00046. Spatially, the largest negative trend was observed in the north-western part of the Province, whereas the largest positive trend was observed in the southern parts.

3.2. Trends in NDVI and SVI during El Niño events

Similar to the rainfall and SPI, the NDVI and SVI showed an increase in drought intensity during aggressive droughts and a decrease in drought intensity during regressive droughts. That is, during droughts in which moderate or strong El Niño conditions prevailed, the drought severity decreased as the season progressed, whereas during droughts in which El Niño conditions were absent or weak, the drought severity increased over time. Considering the 2001/2002 and 2015/2016 rainfall seasons, the characteristics of aggressive and regressive droughts, respectively, were observed. In the 2001/2002 season, the SVI was 1.59 on 17 November 2001 and decreased to 1.16 on 3 December 2001. The SVI continued to decrease steadily throughout the season until it reached a low of −2.30 on 22 March 2002. Similarly, the NDVI decreased from 0.55 on 17 January 2002 to 0.46 on 22 March 2002. In contrast, as the 2015/2016 rainfall season progressed, the SVI and NDVI increased. In particular, the SVI decreased from −0.68 on 17 November 2015 to a low of −1.50 on 1 January 2016 and then increased to 0.64 on 21 March 2016. Meanwhile, the NDVI increased from 0.33 on 17 November 2015 to 0.69 on 21 March 2016. Over the entire MODIS data study period, notable decreases in NDVI and SVI were observed during the rainfall seasons of 2001/2002, 2002/2003, 2004/2005, 2013/2014, 2015/2016, and 2019/2020 (Figure 6).

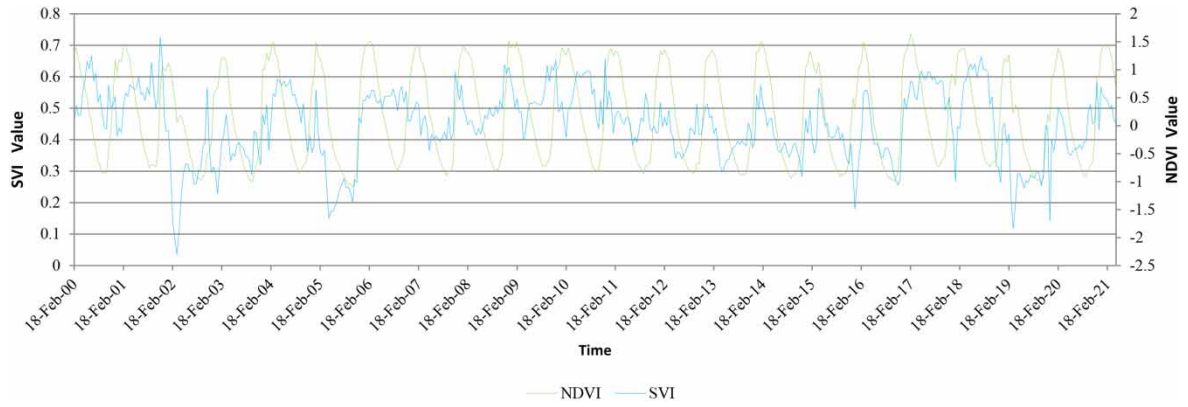

Figure 6 | Changes in 16-day NDVI and SVI from February 2000 to April 2021 over the Southern Province of Zambia.

The results of the Mann–Kendall trend tests for the NDVI revealed that Southern Province experienced an upward trend in the western and southern parts (agroecological Region I) and a downward trend in the central

plateau area (agroecological Region II). The magnitude of these trends was much higher for NDVI than for SPI, as the NDVI slope medians ranged from −0.983 to 1.269 (Figure 7), whereas the SPI slope medians ranged from 0.00052 to 0.00046. The Mann–Kendall trend test results for the SVI were similar to those for the NDVI in that downward trends were detected in the central plateau of the province, whereas an upward trend was detected in the western and southern parts. However, the magnitudes of the SVI trends were smaller than those of the NDVI, as the SVI slope medians ranged from −0.00069 to 0.00068. Despite the small range of the SVI slope medians, the range was still higher than that of the SPI.

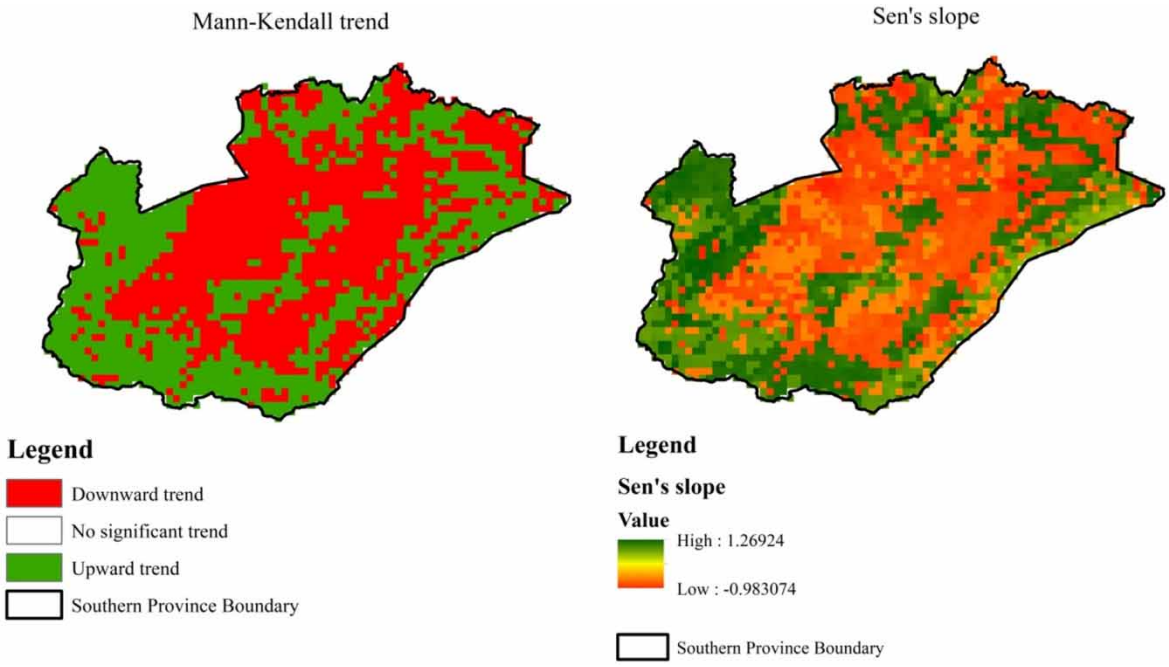

Figure 7 | Mann–Kendall trend test and Sen's slope of NDVI for the Southern Province of Zambia.

The higher magnitudes of certain trends (and hence, change) can be attributed mainly to changes in land cover and land use and only partially to climate change. This was evidenced by the larger ranges of slope medians in the vegetation indices than in the SPI. Changes in land cover and land use occur at a faster rate than changes in climate. Although climate change is a slow and steady process, land cover and land use changes can occur abruptly as forests, grasslands, wetlands, and other vegetated land cover types are converted into agricultural fields, urban areas, and other anthropogenically dominated landscapes. Notably, Southern Province is one of the main hotspots of deforestation in Zambia due to agricultural expansion, infrastructure development, wood extraction, and fires (Vinya *et al.* 2011). Therefore, it has been subject to land use change during the study period.

Although the Mann–Kendall trend test and Sen's slope method yielded similar results for the NDVI and SVI, there was still a large difference in the ranges of the slope medians. The smaller range of the SVI may have been attributable to it being an indicator of the deviations of the vegetation condition at a specific time from the mean vegetation condition in a specific pixel, derived from the *z*-score. The mean vegetation condition of each pixel is influenced by all vegetation conditions over time, and the mean vegetation conditions affect both the past and present values when calculating the SVI. Furthermore, seasonality is absent in the SVI. However, the NDVI value indicates the vegetation condition at a discrete point in time (not relative), and seasonality is present, resulting in larger changes. Additionally, NDVI values are related in one direction of time (when performing trend tests), that is, from the past to the present.

3.3. Prospects for WEF nexus during extreme droughts

Droughts in southern Zambia can be classified into two categories: regressive droughts and aggressive droughts. We determined that regressive droughts coincided with moderate to strong El Niño conditions and were characterised by the decrease in drought intensity as a rainfall season progressed. Aggressive droughts were

characterised by an increase in drought intensity as the season wore in and the absence of moderate to strong El Niño conditions. Recessive droughts tend to dissipate by February and hence rainfall would be available thereafter. We postulate that this is likely the case for the Southern Africa. Therefore, even though El Niño events greatly undermine water security, it means delayed planting to ensure maximum crop productive during strong El Niño events. Soil moisture also tends to be adequate to support the vegetation cover. Further investigations are required to evaluate variability in both evaporation and soil moisture over this region as demonstrated by studies such as Gushchina *et al.* (2020). However, during the weak to moderate El Niño events, the droughts seem to be persistent. Investigations are therefore required to determine suitable sites for other technologies such as managed aquifer recharge (MAR). MAR would provide a better climate buffer in the region and assure water security under water stress. Drought-prone areas such as Southern Zambia have a number of dams, however, storage capacity of these dams require further investigation due to the burden of sediments (Winton *et al.* 2021). Furthermore, this region tends to have high evaporation rates (Hamududu & Ngoma 2020). Rainwater harvesting would be an option for the urbanised parts of the region although limited due to spatial variability.

Provided that water is conveyed to agricultural fields/farms, energy (electricity) provision must be assured to support food security amid climate extremes, such as droughts (Taguta *et al.* 2022). A water–energy–food (WEF) nexus framework is required to respond to drivers of change, such as climate variability and change. The WEF nexus is broadly defined as an approach that considers the interactions, synergies, and trade-offs of WEF when managing these resources (Mabhaudhi *et al.* 2016; Ololade *et al.* 2017; Nhamo *et al.* 2020). WEF securities are inextricably linked, with usage within one sector influencing use and availability in adjacent sectors. Unlike Integrated Water Resource Management (IWRM), which is water-centric in nature, the goal of the WEF nexus is to approach resource management more holistically using a multi-centric philosophy. The WEF nexus presents an opportunity for different actors to integrate sectors to optimise the use of the resource base, maximise synergies, and minimise trade-offs and conflicts.

Several studies have proposed various WEF frameworks. Ringler *et al.* (2013) presented the concept of the water–energy–land and food (WELF) nexus. The WELF nexus framework evaluates the linkages among the water, energy, land, and food sectors. The direct and indirect drivers of change affecting these linkages are clearly depicted in the framework. Conway *et al.* (2015) examined Southern Africa's nexus from the perspective of climate and a modified Hoff's nexus framework (Hoff 2011), which integrates global trends (drivers) with fields of action, to highlight the role of climate as a driver. The framework in this study considered the main elements of intra-regional links that occur in WEF sectors at a national level, while highlighting connections at the river basin scale and drawing attention to case studies of many examples of specific trade-offs and synergies.

Smajgl *et al.* (2016) presented a sectorally balanced, dynamic WEF nexus framework in which sectoral objectives were given equal weightings. The analyses show that this type of framework reveals the emergence and/or changes in cross-sectoral connections because of single-sector interventions. Karabulut *et al.* (2018) proposed a synthesis matrix system that describes the complex and closely related relationships between the natural resources used for food (specifically water and land), energy (defined as ecosystem service flows in the matrix system), and ecosystems within the WELF concept. The matrix system can be defined at different scales (from global to local) and includes the impacts and nexuses of climate change. Martinez-Hernandez *et al.* (2017) proposed a simulation and analytics framework and a concomitant Nexus Simulation System termed 'NexSym'. This study aimed to develop a framework or tool for integrated resource assessment, accounting for integration within and across WEF sectors, ecosystems, and consumption components that interact with a local system. Martinez-Hernandez *et al.* (2017) indicated that there is a need for a nexus tool on a local scale as solutions are better tailored to local conditions and it becomes easier to achieve synergistic techno-ecological interactions.

Recent studies on WEF nexus implementation in the context of developing countries have shown that key societal problems at a local scale that affect livelihoods are weakly considered, such as energy sources, education status, land issues, and nutrition compounded with data scarcity issues, combined with 'top-down' approaches (Olawuyi 2020; Naidoo *et al.* 2021; Kabeya *et al.* 2022; Taguta *et al.* 2022). Based on these shortcomings and the findings of this study, a new adaptive framework is proposed, as shown in Figure 8. The framework combines a mix of different frameworks with an emphasis on innovations that should be used to operationalise WEF in the wake of climate variability and change in a local context. Some of these technologies include inter-basin transfer schemes, MAR, and the use of renewable energy. Innovation must be supported by a commitment to an enabling environment and financing from a governance perspective.

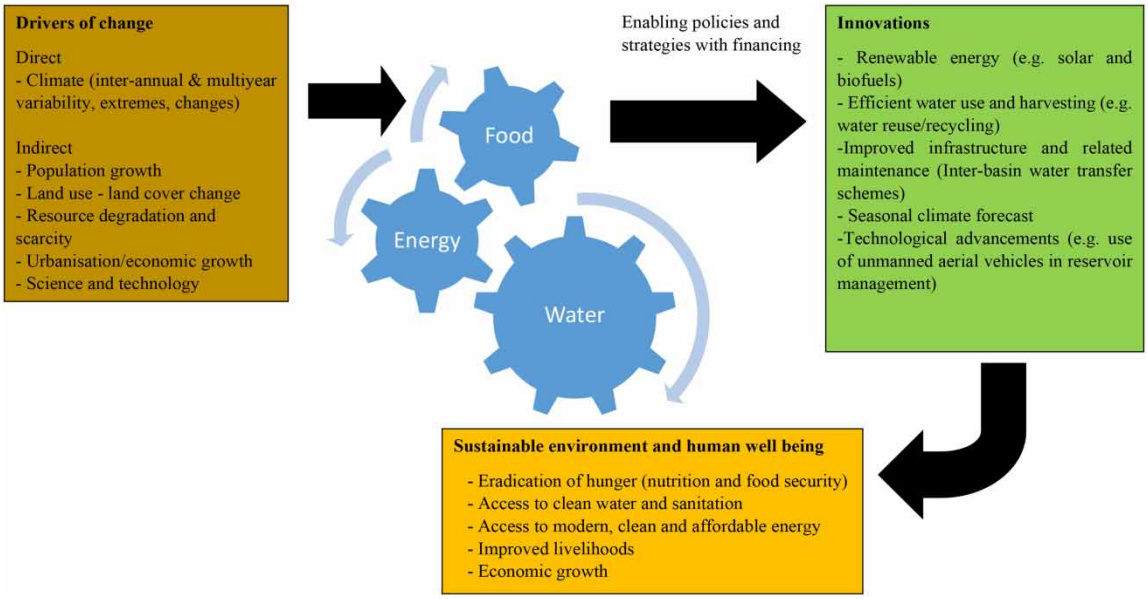

Figure 8 | Proposed WEF nexus in the context of climate dynamics.

4. CONCLUSION

This study demonstrated that droughts in Southern Province, Zambia are generally aggressive; however, during strong El Niño events, they tend to be regressive. Regressive droughts dissipated by February; subsequently, precipitation ensured water availability, as demonstrated by the SPI. Further investigation of vegetation cover using SVI showed that during El Niño events, vegetation cover tends to be resilient owing to residual soil moisture. Further investigation is required to evaluate the dynamics of vegetation cover in relation to soil moisture across regions. The SPI and SVI are appropriate for tracking the onset, development, and termination of droughts induced by ENSO in this region. Furthermore, this study demonstrated that water and food security must be achieved using a WEF nexus approach. Innovations such as MAR and renewable energy options must be used for sustainable resource utilisation. In addition, delayed planting coinciding with an increase in rainfall during regressive droughts is a potential strategy for ensuring food security. The results of this study elucidate the trends in drought during El Niño events and serve as a valuable reference for drought adaptation strategies. Using the WEF nexus approach, prospects for sustainable environmental management and improved livelihoods should be investigated using a modelling framework in the future.

ACKNOWLEDGEMENTS

This work received support from the Tipping Points Explained by Climate Change Project with funding from SASSCAL (The Southern African Science Service Centre for Climate Change and Adaptive Land Management). Partial funding was also received from NEPAD-SANWATCE and implemented through the WAFSA Fund.

DATA AVAILABILITY STATEMENT

All relevant data are included in the paper or its Supplementary Information.

CONFLICT OF INTEREST

The authors declare there is no conflict.

REFERENCES

Arab, S. T. & Ahamed, T. (2023) Near-real-time drought monitoring and assessment for vineyard production on a regional scale with standard precipitation and vegetation indices using Landsat and CHIRPS datasets, *Asia-Pacific Journal of Regional Science*, **7**, 591–614. doi:10.1007/s41685-023-00286-7.

Asadi-Zarch, M. A., Sivakumar, B. & Sharma, A. (2015) Droughts in a warming climate: A global assessment of standardized precipitation index (SPI) and reconnaissance drought index (RDI), *Journal of Hydrology*, **526**, 183–195. https://doi.org/10.1016/j.jhydrol.2014.09.071.

Ayugi, B., Eresanya, E. O., Onyango, A. O., Ogou, F. K., Okoro, E. C., Okoye, C. O., Anoruo, C. M., Dike, V. N., Ashiru, O. R., Daramola, M. T., Mumo, R. & Ongoma, V. (2022) Review of meteorological drought in Africa: Historical trends, impacts, mitigation measures, and prospects, *Pure and Applied Geophysics*, **179**, 1365–1386. doi:10.1007/s00024-022-02988-z.

Bhuiyan, C., Singh, R. P. & Kogan, F. N. (2006) Monitoring drought dynamics in the Aravalli region (India) using different indices based on ground and remote sensing data, *International Journal of Applied Earth Observation and Geoinformation*, **8**, 289–302. https://doi.org/10.1016/j.jag.2006.03.002.

Bhunia, P., Das, P. & Maiti, R. (2020) Meteorological drought study through SPI in three drought prone districts of West Bengal, *India. Earth Systems and Environment*, **4**, 43–55. doi:10.1007/s41748-019-00137-6.

Bonaccorso, B., Bordi, I., Cancelliere, A., Rossi, G. & Sutera, A. (2003) Spatial variability of drought: An analysis of the SPI in Sicily, *Water Resources Management*, **17**, 273–296. doi:10.1023/A:1024716530289.

Cliggett, L., Colson, E., Hay, R., Scudder, T. & Unruh, J. (2007) Chronic Uncertainty and Momentary Opportunity: A half century of adaptation among Zambia's Gwembe Tonga. *Human Ecology*, **35**, 19–31. 10.1007/s10745-006-9080-7.

Conway, D., van Garderen, E. A., Deryng, D., Dorling, S., Krueger, T., Landman, W., Lankford, B., Lebek, K., Osborn, T., Ringler, C., Thurlow, J., Zhu, T. & Dalin, C. (2015) Climate and Southern Africa's water–energy–food nexus, *Nature Climate Change*, **5**, 837–846. doi:10.1038/nclimate2735.

Dai, A. (2011) Drought under global warming: A review, *WIREs Climate Change*, **2**, 45–65. https://doi.org/10.1002/wcc.81.

Dibi-Anoh, P. A., Koné, M., Gerdener, H., Kusche, J. & N'Da, C. K. (2023) Hydrometeorological extreme events in West Africa: Droughts, *Surveys in Geophysics*, **44**, 173–195. doi:10.1007/s10712-022-09748-7.

Ezzine, H., Bouziane, A. & Ouazar, D. (2014) Seasonal comparisons of meteorological and agricultural drought indices in Morocco using open short time-series data, *International Journal of Applied Earth Observation and Geoinformation*, **26**, 36–48. https://doi.org/10.1016/j.jag.2013.05.005.

Fatras, C., Parrens, M., Peña Luque, S. & Al Bitar, A. (2021) Hydrological dynamics of the Congo basin from water surfaces based on L-Band microwave, *Water Resources Research*, **57**, e2020WR027259. https://doi.org/10.1029/2020WR027259.

Gebrehiwot, T., van der Veen, A. & Maathuis, B. (2011) Spatial and temporal assessment of drought in the northern highlands of Ethiopia, *International Journal of Applied Earth Observation and Geoinformation*, **13**, 309–321. https://doi.org/10.1016/j.jag.2010.12.002.

Ghazaryan, G., Dubovyk, O., Graw, V., Kussul, N. & Schellberg, J. (2020) Local-scale agricultural drought monitoring with satellite-based multi-sensor time-series, *GIScience & Remote Sensing*, **57**, 704–718. doi:10.1080/15481603.2020.1778332.

Gushchina, D., Zheleznova, I., Osipov, A. & Olchev, A. (2020) Effect of various types of ENSO events on moisture conditions in the humid and subhumid tropics, *Atmosphere*, **11**, 1354. doi:10.3390/atmos11121354.

Hamududu, B. H. & Ngoma, H. (2020) Impacts of climate change on water resources availability in Zambia: Implications for irrigation development, *Environment, Development and Sustainability*, **22**, 2817–2838. doi:10.1007/s10668-019-00320-9.

Heim, R. R. (2002) A review of twentieth-century drought indices used in the United States, *Bulletin of the American Meteorological Society*, **83**, 1149–1166. https://doi.org/10.1175/1520-0477-83.8.1149.

Hernández, A. J. J. & Heslar, M. (2019) Examining the spatiotemporal characteristics of droughts in the Caribbean using the standardized precipitation index (SPI), *Climate Research*, **78**, 103–116.

Hoff, H. (2011). Understanding the Nexus. Background paper for Bonn 2011 conference: The water, energy and food security nexus, Stockholm Environment Institute.

IPCC (2014) Climate change 2014: Synthesis report. In: Core Writing Team, Pachauri, R. K. & Meyer, L.A. (eds.) Contribution of Working Groups I, II and III to the Fifth Assessment Report of the Intergovernmental Panel on Climate Change. Geneva, Switzerland, IPCC, pp. 151.

Jain, S. K., Keshri, R., Goswami, A. & Sarkar, A. (2010) Application of meteorological and vegetation indices for evaluation of drought impact: A case study for Rajasthan, India, *Natural Hazards*, **54**, 643–656. doi:10.1007/s11069-009-9493-x.

Ji, L. & Peters, A. J. (2003) Assessing vegetation response to drought in the northern Great Plains using vegetation and drought indices, *Remote Sensing of Environment*, **87**, 85–98. https://doi.org/10.1016/S0034-4257(03)00174-3.

Ji, L. & Peters, A. J. (2005) Lag and seasonality considerations in evaluating AVHRR NDVI response to precipitation, *Photogrammetric Engineering & Remote Sensing*, **71**, 1053–1061. doi:10.14358/PERS.71.9.1053.

Juntakut, P., Jantakat, Y. & Jantakat, C. (2021) Google Earth Engine for monitoring drought impacts on urban tree using the Standardized Vegetation Index (SVI) in Amphoe Mueang, Nakhonratchasima Province, Thailand, *International Journal of Building, Urban, Interior and Landscape Technology (BUILT)*, **18**, 41–54.

Kabeya, P. K., Mndzebele, D., Ntlamelle, M., Samikwa, D., Simalabwi, A., Takawira, A., Jembere, K. & Kumbirai, S. (2022) A regional approach to implementing the WEF nexus: a case study of the Southern African Development Community. In: Mabhaudhi, T., Senzanje, A., Modi, A., Jewitt, G. & Massawe, F. (eds.) Water–Energy–Food Nexus Narratives and Resource Securities. Elsevier, pp. 145–167.

Karabulut, A. A., Crenna, E., Sala, S. & Udias, A. (2018) A proposal for integration of the ecosystem-water-food-land-energy (EWFLE) nexus concept into life cycle assessment: A synthesis matrix system for food security, *Journal of Cleaner Production*, **172**, 3874–3889. https://doi.org/10.1016/j.jclepro.2017.05.092.

Khalili, D., Farnoud, T., Jamshidi, H., Kamgar-Haghighi, A. A. & Zand-Parsa, S. (2011) Comparability analyses of the SPI and RDI meteorological drought indices in different climatic zones, *Water Resources Management*, **25**, 1737–1757. doi:10.1007/s11269-010-9772-z.

Mabhaudhi, T., Mpandeli, S., Madhlopa, A., Modi, A. T., Backeberg, G. & Nhamo, L. (2016) Southern Africa's water–energy nexus: Towards regional integration and development, *Water*, **8**, 235.

Martinez-Hernandez, E., Leach, M. & Yang, A. (2017) Understanding water-energy-food and ecosystem interactions using the nexus simulation tool NexSym, *Applied Energy*, **206**, 1009–1021. https://doi.org/10.1016/j.apenergy.2017.09.022.

McKee, T. B., Doesken, N. J. & Kleist, J. (1993) 'The relationship of drought frequency and duration to time scales', *Proceedings of the 8th conference on applied climatology*, 17–22 January 1993, Anaheim, California.

Mikaili, O. & Rahimzadegan, M. (2022) Investigating remote sensing indices to monitor drought impacts on a local scale (case study: Fars province, Iran), *Natural Hazards*, **111**, 2511–2529. doi:10.1007/s11069-021-05146-1.

Mishra, S. S. & Nagarajan, R. (2011) Spatio-temporal drought assessment in Tel river basin using Standardized Precipitation Index (SPI) and GIS, *Geomatics, Natural Hazards and Risk*, **2**, 79–93. doi:10.1080/19475705.2010.533703.

Morid, S., Smakhtin, V. & Moghaddasi, M. (2006) Comparison of seven meteorological indices for drought monitoring in Iran, *International Journal of Climatology*, **26**, 971–985. https://doi.org/10.1002/joc.1264.

Naidoo, D., Nhamo, L., Mpandeli, S., Sobratee, N., Senzanje, A., Liphadzi, S., Slotow, R., Jacobson, M., Modi, A. T. & Mabhaudhi, T. (2021) Operationalising the water-energy-food nexus through the theory of change, *Renewable and Sustainable Energy Reviews*, **149**, 111416. https://doi.org/10.1016/j.rser.2021.111416.

Nhamo, L., Mabhaudhi, T., Mpandeli, S., Dickens, C., Nhemachena, C., Senzanje, A., Naidoo, D., Liphadzi, S. & Modi, A. T. (2020) An integrative analytical model for the water-energy-food nexus: South Africa case study, *Environmental Science & Policy*, **109**, 15–24. https://doi.org/10.1016/j.envsci.2020.04.010.

Niang, I., Ruppel, O. C., Abdrabo, M. A., Essel, A., Lennard, C., Padgham, J. & Urquhart, P. (2014) Climate change 2014: Impacts, adaptation and vulnerability. Part B: Regional aspects. In: *Working Group II Contribution to the Fifth Assessment Report of the Intergovernmental Panel on Climate Change*, pp. 1199–1266.

Nikraftar, Z., Mostafaie, A., Sadegh, M., Afkueieh, J. H. & Pradhan, B. (2021) Multi-type assessment of global droughts and teleconnections, *Weather and Climate Extremes*, **34**, 100402. https://doi.org/10.1016/j.wace.2021.100402.

NOAA (2022) *Climate Variability: Oceanic Niño Index* [Online]. Internet: Climate Prediction Center – ONI. Available at: http://origin.cpc.ncep.noaa.gov/products/analysis_monitoring/ensostuff/ONI_v5.php [Accessed 7th May 2022].

Olawuyi, D. (2020) Sustainable development and the water-energy-food nexus: Legal challenges and emerging solutions, *Environmental Science & Policy*, **103**, 1–9. https://doi.org/10.1016/j.envsci.2019.10.009.

Ololade, O. O., Esterhuyse, S. & Levine, A. D. (2017) *The Water-Energy-Food Nexus from a South African Perspective. In Water-Energy-Food Nexus* (Salam, P. A., Shrestha, S., Pandey, V. P. & Anal, A. K., eds). Wiley, pp. 127–140.

Peters, A. J., Walter-Shea, E. A., Ji, L., Viña, A., Hayes, M. & Svoboda, M. D. (2002) Drought monitoring with NDVI-based Standardised Vegetation Index, *Photogrammetric Engineering and Remote Sensing*, **68**, 71–75.

Pomposi, C., Funk, C., Shukla, S., Harrison, L. & Magadzire, T. (2018) Distinguishing Southern Africa precipitation response by strength of El Niño events and implications for decision-making, *Environmental Research Letters*, **13**, 074015.

Raposo, V. d. M. B., Costa, V. A. F. & Rodrigues, A. F. (2023) A review of recent developments on drought characterization, propagation, and influential factors, *Science of The Total Environment*, **898**, 165550. https://doi.org/10.1016/j.scitotenv.2023.165550.

Ringler, C., Bhaduri, A. & Lawford, R. (2013) The nexus across water, energy, land and food (WELF): Potential for improved resource use efficiency? *Current Opinion in Environmental Sustainability*, **5**, 617–624. https://doi.org/10.1016/j.cosust.2013.11.002.

Sen, P. K. (1968) Estimates of the regression coefficient based on Kendall's Tau, *Journal of the American Statistical Association*, **63**, 1379–1389.

Smajgl, A., Ward, J. & Pluschke, L. (2016) The water–food–energy nexus – Realising a new paradigm, *Journal of Hydrology*, **533**, 533–540. https://doi.org/10.1016/j.jhydrol.2015.12.033.

Souza, A. G. S. S., Neto, A. R., Rossato, L., Alvalá, R. C. S. & Souza, L. L. (2018) Use of SMOS L3 soil moisture data: Validation and drought assessment for Pernambuco State, Northeast Brazil, *Remote Sensing*, **10**, 1314.

Souza, A. G. S. S., Ribeiro Neto, A. & Souza, L. L. d. (2021) Soil moisture-based index for agricultural drought assessment: SMADI application in Pernambuco State-Brazil, *Remote Sensing of Environment*, **252**, 112124. https://doi.org/10.1016/j.rse.2020.112124.

Stricevic, R., Djurovic, N. & Djurovic, Z. (2011) Drought classification in Northern Serbia based on SPI and statistical pattern recognition, *Meteorological Applications*, **18**, 60–69. doi:10.1002/met.207.

Taguta, C., Senzanje, A., Kiala, Z., Malota, M. & Mabhaudhi, T. (2022) Water-energy-food nexus tools in theory and practice: A systematic review, *Frontiers in Water*, **4**. doi:10.3389/frwa.2022.837316.

Tam, B., Bonsal, B., Zhang, X., Zhang, Q. & Rong, R. (2023) Assessing potential evapotranspiration methods in future drought projections across Canada, *Atmosphere-Ocean*, 1–13. doi:10.1080/07055900.2023.2288632.

Taye, M. T. & Dyer, E. (2024) Hydrologic extremes in a changing climate: A review of extremes in East Africa, *Current Climate Change Reports*, **10**, 1–11. doi:10.1007/s40641-024-00193-9.

Thavorntam, W., Tantemsapya, N. & Armstrong, L. (2015) A combination of meteorological and satellite-based drought indices in a better drought assessment and forecasting in Northeast Thailand, *Natural Hazards*, **77**, 1453–1474. doi:10.1007/s11069-014-1501-0.

Thenkabail, P. S., Gamage, M. S. & Smakhtin, V. U. (2004) *The Use of Remote-Sensing Data for Drought Assessment and Monitoring in Southwest Asia*. Colombo.

Van Loon, A. F., Gleeson, T., Clark, J., Van Dijk, A. I. J. M., Stahl, K., Hannaford, J., Di Baldassarre, G., Teuling, A. J., Tallaksen, L. M., Uijlenhoet, R., Hannah, D. M., Sheffield, J., Svoboda, M., Verbeiren, B., Wagener, T., Rangecroft, S., Wanders, N. & Van Lanen, H. A. J. (2016) Drought in the Anthropocene, *Nature Geoscience*, **9**, 89–91. doi:10.1038/ngeo2646.

Vinya, R., Kasumu, E., Syampungani, S., Monde, C. & Kasubika, R. (2011) Preliminary Study on the Drivers of Deforestation and Potential for REDD+ in Zambia. A consultancy report prepared for Forestry Department and FAO under the national UN-REDD+ Programme. Lusaka.

Waldman, K. B., Vergopolan, N., Attari, S. Z., Sheffield, J., Estes, L. D., Caylor, K. K. & Evans, T. P. (2019) Cognitive biases about climate variability in smallholder farming systems in Zambia, *Weather, Climate, and Society*, **11**, 369–383. https://doi.org/10.1175/WCAS-D-18-0050.1.

West, H., Quinn, N. & Horswell, M. (2019) Remote sensing for drought monitoring & impact assessment: Progress, past challenges and future opportunities, *Remote Sensing of Environment*, **232**, 111291. https://doi.org/10.1016/j.rse.2019.111291.

Wilhite, D. A. & Glantz, M. H. (1985) Understanding: the drought phenomenon: the role of definitions. *Water international* **10** (3), 111–120.

Wilhite, D. A., Hayes, M. J., Svoboda, M. D., (2000) In: Vogt, J. V. & Somma, F. (eds.) *Drought and Drought Mitigation in Europe*. Dordrecht: Springer Netherlands, pp. 149–160.

Winton, R. S., Teodoru, C. R., Calamita, E., Kleinschroth, F., Banda, K., Nyambe, I. & Wehrli, B. (2021) Anthropogenic influences on Zambian water quality: Hydropower and land-use change, *Environmental Science: Processes & Impacts*, **23**, 981–994. https://doi.org/10.1039/D1EM00006C.

Wu, H., Svoboda, M. D., Hayes, M. J., Wilhite, D. A. & Wen, F. (2007) Appropriate application of the standardized precipitation index in arid locations and dry seasons, *International Journal of Climatology*, **27**, 65–79. https://doi.org/10.1002/joc.1371.

Zhai, J., Su, B., Krysanova, V., Vetter, T., Gao, C. & Jiang, T. (2010) Spatial variation and trends in PDSI and SPI indices and their relation to streamflow in 10 large regions of China, *Journal of Climate*, **23**, 649–663. https://doi.org/10.1175/2009JCLI2968.1.

Zhang, Q., Li, J., Singh, V. P. & Bai, Y. (2012) SPI-based evaluation of drought events in Xinjiang, China, *Natural Hazards*, **64**, 481–492. doi:10.1007/s11069-012-0251-0.

Zhang, X., Li, M., Ma, Z., Yang, Q., Lv, M. & Clark, R. (2019) Assessment of an evapotranspiration deficit drought index in relation to impacts on ecosystems, *Advances in Atmospheric Sciences*, **36**, 1273–1287. doi:10.1007/s00376-019-9061-6.

First received 13 June 2023; accepted in revised form 1 September 2024. Available online 12 September 2024